β-Decay Half-Lives of 110 Neutron-Rich Nuclei across the $N = 82$ Shell Gap: Implications for the Mechanism and Universality of the Astrophysical r Process

G. Lorusso,[1,2,3] S. Nishimura,[1,4] Z. Y. Xu,[1,5,6] A. Jungclaus,[7] Y. Shimizu,[1] G. S. Simpson,[8] P.-A. Söderström,[1] H. Watanabe,[1,9] F. Browne,[1,10] P. Doornenbal,[1] G. Gey,[1,8] H. S. Jung,[11] B. Meyer,[12] T. Sumikama,[13] J. Taprogge,[1,7,14] Zs. Vajta,[1,15] J. Wu,[1,16] H. Baba,[1] G. Benzoni,[17] K. Y. Chae,[18] F. C. L. Crespi,[17,19] N. Fukuda,[1] R. Gernhäuser,[20] N. Inabe,[1] T. Isobe,[1] T. Kajino,[4,21] D. Kameda,[1] G. D. Kim,[22] Y.-K. Kim,[22,23] I. Kojouharov,[24] F. G. Kondev,[25] T. Kubo,[1] N. Kurz,[24] Y. K. Kwon,[22] G. J. Lane,[26] Z. Li,[16] A. Montaner-Pizá,[27] K. Moschner,[28] F. Naqvi,[29] M. Niikura,[5] H. Nishibata,[30] A. Odahara,[30] R. Orlandi,[31] Z. Patel,[3] Zs. Podolyák,[3] H. Sakurai,[1,5] H. Schaffner,[24] P. Schury,[1] S. Shibagaki,[4,21] K. Steiger,[20] H. Suzuki,[1] H. Takeda,[1] A. Wendt,[28] A. Yagi,[30] and K. Yoshinaga[32]

[1]*RIKEN Nishina Center, 2-1 Hirosawa, Wako-shi, Saitama 351-0198, Japan*
[2]*National Physical Laboratory, Teddington, Middlesex TW11 0LW, United Kingdom*
[3]*Department of Physics, University of Surrey, Guildford GU2 7XH, United Kingdom*
[4]*Division of Theoretical Astronomy, NAOJ, 181-8588 Mitaka, Japan*
[5]*Department of Physics, University of Tokyo, Hongo, Bunkyo-ku, Tokyo 113-0033, Japan*
[6]*Department of Physics, the University of Hong Kong, Pokfulam Road, Hong Kong*
[7]*Instituto de Estructura de la Materia, CSIC, E-28006 Madrid, Spain*
[8]*LPSC, Université Joseph Fourier Grenoble 1, CNRS/IN2P3, Institut National Polytechnique de Grenoble, F-38026 Grenoble Cedex, France*
[9]*IRCNPC, School of Physics and Nuclear Energy Engineering, Beihang University, Beijing 100191, China*
[10]*School of Computing, Engineering and Mathematics, University of Brighton, Brighton BN2 4JG, United Kingdom*
[11]*Department of Physics, Chung-Ang University, Seoul 156-756, Republic of Korea*
[12]*Department of Physics and Astronomy, Clemson University, Clemson, South Carolina 29634, USA*
[13]*Department of Physics, Tohoku University, Aoba, Sendai, Miyagi 980-8578, Japan*
[14]*Departamento de Física Teórica, Universidad Autónoma de Madrid, E-28049 Madrid, Spain*
[15]*Institute for Nuclear Research, Hungarian Academy of Sciences, P. O. Box 51, Debrecen H-4001, Hungary*
[16]*Department of Physics, Peking University, Beijing 100871, China*
[17]*INFN Sezione di Milano, I-20133 Milano, Italy*
[18]*Department of Physics, Sungkyunkwan University, Suwon 440-746, Republic of Korea*
[19]*Dipartimento di Fisica, Università di Milano, I-20133 Milano, Italy*
[20]*Physik Department E12, Technische Universität München, D-85748 Garching, Germany*
[21]*Department of Astronomy, University of Tokyo, Hongo, Bunkyo-ku, Tokyo 113-0033, Japan*
[22]*Institute for Basic Science, Rare Isotope Science Project, Yuseong-daero 1689-gil, Yuseong-gu, 305-811 Daejeon, Republic of Korea*
[23]*Department of Nuclear Engineering, Hanyang University, Seoul 133-791, Republic of Korea*
[24]*GSI Helmholtzzentrum für Schwerionenforschung GmbH, 64291 Darmstadt, Germany*
[25]*Nuclear Engineering Division, Argonne National Laboratory, Argonne, Illinois 60439, USA*
[26]*Department of Nuclear Physics, R.S.P.E., Australian National University, Canberra, Australian Capital Territory 0200, Australia*
[27]*Instituto de Física Corpuscular, CSIC-University of Valencia, E-46980 Paterna, Spain*
[28]*Institut für Kernphysik, Universität zu Köln, Zülpicher Strasse 77, D-50937 Köln, Germany*
[29]*Wright Nuclear Structure Laboratory, Yale University, New Haven, Connecticut 06520-8120, USA*
[30]*Department of Physics, Osaka University, Machikaneyama-machi 1-1, Osaka 560-0043 Toyonaka, Japan*
[31]*Instituut voor Kern en Stralingsfysica, KU Leuven, University of Leuven, B-3001 Leuven, Belgium*
[32]*Department of Physics, Tokyo University of Science, 2641 Yamazaki, Noda, Chiba 278-8510, Japan*

(Received 14 October 2014; revised manuscript received 28 January 2015; published 11 May 2015)

The β-decay half-lives of 110 neutron-rich isotopes of the elements from $_{37}$Rb to $_{50}$Sn were measured at the Radioactive Isotope Beam Factory. The 40 new half-lives follow robust systematics and highlight the persistence of shell effects. The new data have direct implications for r-process calculations and reinforce the notion that the second ($A \approx 130$) and the rare-earth-element ($A \approx 160$) abundance peaks may result from the freeze-out of an $(n,\gamma) \rightleftarrows (\gamma,n)$ equilibrium. In such an equilibrium, the new half-lives are important factors determining the abundance of rare-earth elements, and allow for a more reliable discussion of the

r process universality. It is anticipated that universality may not extend to the elements Sn, Sb, I, and Cs, making the detection of these elements in metal-poor stars of the utmost importance to determine the exact conditions of individual r-process events.

DOI: 10.1103/PhysRevLett.114.192501 PACS numbers: 23.40.-s, 26.30.Hj, 27.60.+j

Introduction.—The origin of the heavy elements from iron to uranium is one of the main open questions in science. The slow neutron-capture (s) process of nucleosynthesis [1,2], occurring primarily in helium-burning zones of stars, produces about half of the heavy element abundance in the universe. The remaining half requires a more violent process known as the rapid neutron-capture (r) process [3–6]. During the r process, in environments of extreme temperatures and neutron densities, a reaction network of neutron captures and β decays synthesizes very neutron-rich isotopes in a fraction of a second. These isotopes, upon exhaustion of the supply of free neutrons, decay into the stable or semistable isotopes observed in the solar system. However, none of the proposed stellar models, including explosion of supernovae [7–12] and merging neutron stars [13–16], can fully explain abundance observations. The mechanism of the r process is also uncertain. At temperatures of one billion degrees or more, photons can excite unstable nuclei which then emit neutrons, thus, counteracting neutron captures in an $(n,\gamma) \rightleftarrows (\gamma,n)$ equilibrium that determines the r process. These conditions may be found in the neutrino-driven wind following the collapse of a supernova core and the accreting torus formed around the black hole remnant of merging neutron stars. Alternatively, recent r-process models have shown that the r process is also possible at lower temperatures or higher neutron densities where the contribution from (γ,n) reactions is minor. These conditions are expected in supersonically expanding neutrino-driven outflow in low-mass supernovae progenitors (e.g., $8-12\,M_{\odot}$) or prompt ejecta from neutron star mergers [17]. The final abundance distribution may also be dominated by post-processing effects such as fission of heavy nuclei ($A \gtrsim 280$) possibly produced in merging neutron stars [18].

New clues about the r process have come from the discovery of detailed elemental distributions in some metal-poor stars in the halo of our galaxy [19,20]. A main conclusion of these observations is that the abundance pattern of the elements between barium (Ba, proton number $Z = 56$) and hafnium (Hf, $Z = 78$) is universal. Recent observations by the Space Telescope Imaging Spectrograph on board of the Hubble Space Telescope [21,22] indicate that tellurium (Te, $Z = 52$) is also robustly produced along with the rare earth elements.

Nuclear physics properties such as β-decay half-lives and masses are key for predicting abundance patterns and extract signatures of the r process from a detailed comparison to astronomical observations [23]. This is especially true when $(n,\gamma) \rightleftarrows (\gamma,n)$ equilibrium is established. Otherwise, (n,γ) cross sections or fission properties may very well be responsible for main features of the abundance observations. In this Letter, we report on the half-life measurement of 110 unstable nuclei with proton number $Z \leq 50$ and neutron number $N \approx 82$. These nuclei are key in any r-process mechanism [23] because their enhanced binding bends the r-process path closer to stability slowing down the reaction flow—the flow has to wait at the slowly decaying species. The half-lives of these waiting-point nuclei determine the time scale of the r process and shape the prominent r-process abundance peak of isotopes with $A \approx 130$. The precise theoretical prediction of these half-lives is challenging because the structure evolution of $N \approx 82$ nuclei is still unknown despite the recent experimental efforts [24–30]. The data we present in this Letter also serve as important constraints to probe and improve nuclear models in this region.

Experimental procedure.—The nuclei of interest were produced by fission of a ^{238}U beam induced through collisions with a beryllium target. The U beam had an energy of 345A MeV and an average intensity of about 6×10^{10} ions/s. After selection and identification, exotic nuclei were implanted at a rate of 50 ions/s in the stack of

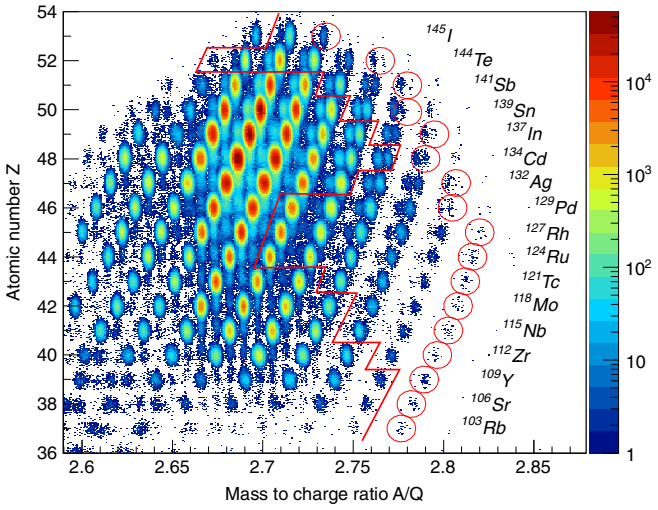

FIG. 1 (color online). Particle identification spectrum [33]. Ions are identified with respect to proton number Z and the mass-to-charge ratio A/Q. Charge state contamination is significant but well separated in A/Q for the nuclei of interest. Nuclei with newly measured half-lives are on the right side of the red solid line. The heaviest masses for which half-lives can be measured are tagged for reference by red circles. The half-lives reported in this Letter are for the elements from Rb to Sn.

eight double-sided silicon strip detectors WAS3ABi [31], surrounded by the 84 high-purity germanium detectors of the EURICA array [32] to detect γ radiation from the excited reaction products. The particle identification spectrum of the isotopes delivered to the decay station is shown in Fig. 1. Implanted ions and subsequent electrons emitted in the ions' β decays were correlated in time and position to build decay curves and extract half-lives using the analysis method detailed in Ref. [34].

Results and discussion.—The resulting half-life measurements are reported in Table I, and illustrated in Fig. 2, compared with previous measurements and with the predictions of several theoretical models. The experimental half-lives follow very regular trends, as expected phenomenologically in nuclei with large Q values [36], but with the noticeable feature that the odd-even staggering of half-lives is weakened crossing the $N = 82$ shell gap (see Fig. 2). This is a signature of the shell structure of atomic nuclei and of the neutron-neutron pairing interaction, which is stronger in $N \leq 82$ nuclei (valence neutrons in the $h_{11/2}$ orbit) than in $N > 82$ nuclei (valence neutrons in the $f_{7/2}$ orbit). This effect should be more evident in the Q-value trends, as predicted in Ref. [37]. It is also clear that crossing the large $N = 82$ shell gap does not produce discontinuities in the half-life trends. These systematics, partially obscured in previous literature data probably by systematic errors, are now firmly established for In, Cd, Ag, and Pd isotopes, and can be interpreted by quasiparticle random-phase approximation (QRPA) calculation as in Refs. [37–39]. In $N > 82$ nuclei, the ground state to ground state transition $\nu f_{7/2} \rightarrow \pi g_{9/2}$ is a first forbidden decay, and the Gamow-Teller (GT) transition $\nu f_{7/2} \rightarrow \pi f_{5/2}$ is largely blocked by the almost complete occupancy of the $\pi f_{5/2}$ orbital. The main GT-decay branch is $\nu g_{7/2} \rightarrow \pi g_{9/2}$, which populates excited states of daughter nuclei. Thus, the isobaric mass difference is not directly reflected in the Q value available for β decay. The half-life trends of In, Cd, and Ag isotopes agree very well with the Fayans energy-density-functional (DF3) + continuum QRPA (CQRPA) model predictions [37], which are applicable for nearly spherical nuclei—In, Cd, and Ag isotopes are, indeed, expected to be spherical, based on several mass models. The agreement worsens for non-closed-shell isotopes of lighter elements, suggesting that deformation in these isotopic chains is not negligible. The data presented here is important for the future development of the DF3 + CQRPA model and its extension to nonspherical nuclei. Discrepancies by a factor of 3–4 between experimental half-lives and predictions of global models such as finite-range droplet model (FRDM) + QRPA [40] already observed for the more stable isotopes, persist further from stability. However, the general trend of FRDM + QRPA and experimental values is very similar, despite a systematic overestimation. This suggests a continuity of mass and decay properties between the studied nuclei and the previously known less exotic ones. Based on this comparison to theoretical models, we conclude that the

TABLE I. Half-lives measured in the present work.

Nucleus	Half-life (ms)	Nucleus	Half-life (ms)	Nucleus	Half-life (ms)	Nucleus	Half-life (ms)	Nucleus	Half-life (ms)
^{134}Sn	890(20)	^{132}Cd	82(4)	^{119}Rh	190(6)	^{116}Tc	57(3)	^{113}Nb	32(4)
^{135}Sn	515(5)	^{133}Cd	64(8)	^{120}Rh	131(5)	^{117}Tc	44.5(30)	^{114}Nb	17(5)
^{136}Sn	350(5)	^{134}Cd	65(15)	^{121}Rh	76(5)	^{118}Tc	30(4)	^{115}Nb	23(8)
^{137}Sn	230(30)	^{124}Ag	180(3)	^{122}Rh	51(6)	^{119}Tc	22(3)	^{106}Zr	175(7)
^{138}Sn	140^{+30}_{-20}	^{125}Ag	150(8)	^{123}Rh	42(4)	^{120}Tc	21(5)	^{107}Zr	150(3)
^{139}Sn	130(60)	^{126}Ag	98(5)	^{124}Rh	30(2)	^{121}Tc	22(6)	^{108}Zr	785(2)
^{128}In	810(30)	^{127}Ag	89(2)	^{125}Rh	26.5(20)	^{109}Mo	700^{+40}_{-60}	^{109}Zr	56(3)
^{129}In	570(10)	^{128}Ag	59(5)	^{126}Rh	19(3)	^{110}Mo	292(7)	^{110}Zr	37.5(20)
^{130}In	284(10)	^{129}Ag	52(4)	^{127}Rh	20^{+20}_{-7}	^{111}Mo	196(5)	^{111}Zr	24.0(5)
^{131}In	261(3)	^{130}Ag	42(5)	^{116}Ru	204(6)	^{112}Mo	125(5)	^{112}Zr	30^{+30}_{-10}
^{132}In	198(2)	^{131}Ag	35(8)	^{117}Ru	151(3)	^{113}Mo	80(2)	^{104}Y	198(20)
^{133}In	163(7)	^{132}Ag	28^{+15}_{-12}	^{118}Ru	99(3)	^{114}Mo	58(2)	^{105}Y	107^{+6}_{-9}
^{134}In	126(7)	^{121}Pd	290(1)	^{119}Ru	69.5(20)	^{115}Mo	45.5(20)	^{106}Y	82^{+10}_{-5}
^{135}In	103(5)	^{122}Pd	195(5)	^{120}Ru	45(2)	^{116}Mo	32(4)	^{107}Y	33.5(3)
^{136}In	85^{+10}_{-8}	^{123}Pd	108(1)	^{121}Ru	29(2)	^{117}Mo	22(5)	^{108}Y	30(5)
^{137}In	65^{+40}_{-30}	^{124}Pd	88(15)	^{122}Ru	25(1)	^{118}Mo	19^{+7}_{-4}	^{109}Y	25(5)
^{126}Cd	513(6)	^{125}Pd	57(10)	^{123}Ru	19(2)	^{107}Nb	280(20)	^{103}Sr	53(10)
^{127}Cd	330(20)	^{126}Pd	48.6(8)	^{124}Ru	15(3)	^{108}Nb	195(6)	^{104}Sr	53(5)
^{128}Cd	245(5)	^{127}Pd	38(2)	^{112}Tc	323(6)	^{109}Nb	110(6)	^{105}Sr	39(5)
^{129}Cd	154.5(20)	^{128}Pd	35(3)	^{113}Tc	152(8)	^{110}Nb	82(2)	^{106}Sr	20^{+8}_{-7}
^{130}Cd	127(2)	^{129}Pd	31(7)	^{114}Tc	120(10)	^{111}Nb	54(2)	^{102}Rb	37(10)
^{131}Cd	98.0(2)	^{118}Rh	285(10)	^{115}Tc	78(2)	^{112}Nb	38(2)	^{103}Rb	23^{+13}_{-9}

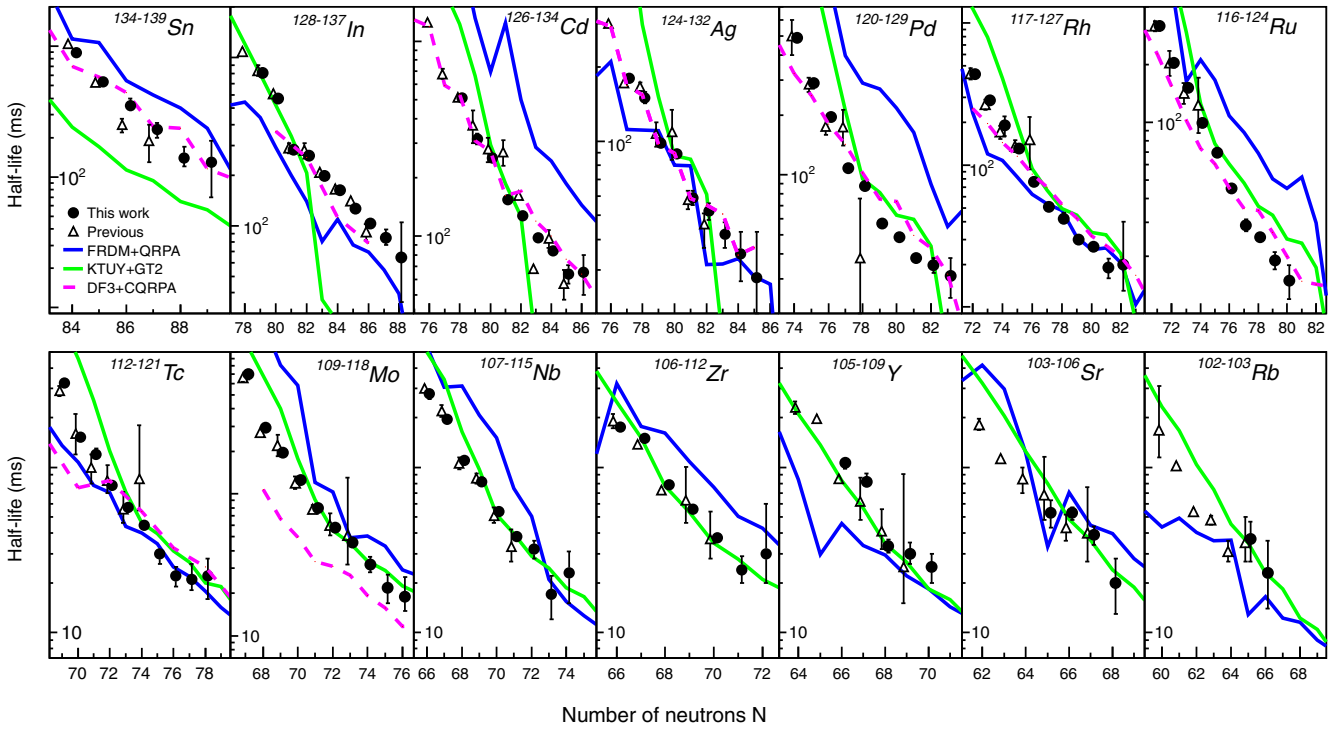

FIG. 2 (color online). β-decay half-lives determined in this work (solid circles) for a number of isotopic chains as a function of neutron number, compared with previous results [35] (open triangles) and the predictions of the models FRDM + QRPA (blue), KTUY + GT2 (green), and DF3 + CQRPA (magenta) when available.

data presented here show no evidence of nuclear structure changes capable of modifying the gross properties of the nuclei we have studied. The sudden drop of half-lives observed of the Koura-Tachibana-Uno-Yamada (KTUY) + GT2 calculations [41,42] when crossing of the $N = 82$ shell is not observed in the data. Since the Q_β values predicted by the KTUY and DF3 mass models are very similar, our data indicate a failure of the second generation of gross theory (GT2) employed to calculate half-lives rather than to the KTUY mass model.

The half-lives of the $N = 82$ nuclei are of particular interest for probing shell model calculations. The tendency to overestimate the half-life of ^{129}Ag reported in Refs. [43,44], persists in the more exotic nuclei ^{128}Pd and ^{127}Rh (see Table II). However, in these calculations, the quenching factor of the GT operator ($q = 0.66$) was chosen to reproduce the half-life of ^{130}Cd (162 ± 7 ms) reported in Ref. [46], which is longer than the one reported here (127 ± 2 ms). The new $N = 82$ half-lives reveal that the calculated values are systematically longer by a nearly constant factor, with the only exception of ^{131}In. Assuming that the decay of $N = 82$ nuclei was dominated by GT transitions [44], such a constant factor could be approximately accounted by a different choice of the GT quenching factor. The value $q = 0.75$ extracted in this way agrees with the systematics of pf-shell nuclei [48] and neutron-deficient nuclei [49]. However, the new half-lives clearly indicate that the proton-hole nucleus ^{131}In is not following the trend expected from the shell-model calculations, an observation that calls for further investigation.

Nucleosynthesis calculations.—The implications of the new half-lives for the r process were investigated by conducting a fully dynamic reaction-network calculation [50,51] study that simulated a spherically symmetric outflow from a neutron-rich stellar environment. The time evolution of matter density followed an early rapid exponential expansion with timescale τ and a later free expansion with a longer timescale approaching a constant velocity [52]. The initial proton-to-neutron ratio was set

TABLE II. Comparison of the present $N = 82$ half-lives with previous measurements and the shell model calculations in Ref. [44].

	Half-Life (ms)		
Nucleus	This work	Previous	Shell Model
^{131}In	261(3)[a]	280(30) [45]	247.53
^{130}Cd	127(2)[b]	162(7) [46]	164.29
^{129}Ag	52(4)	46^{+5}_{-9} [47]	69.81
^{128}Pd	35(3)		47.25
^{127}Rh	20^{+20}_{-7}		27.98

[a]$T_{1/2}$ gated on γ-ray energy 2434 keV.
[b]$T_{1/2}$ gated on γ-ray energies 451, 1669, and 1171 keV.

through the electron fraction Y_e, which, for matter consisting only of free neutrons n and protons p, is $Y_e = p/(n+p)$. In case of exploding stars, different mass zones (a star's layers of different density) have different initial entropy S, so that an explosion was simulated as a superposition of entropy components as in Refs. [53,54]. Given the large uncertainties in current stellar hydrodynamical simulations, none of the above parameters was fixed to specific values. We choose, instead, to use a site-independent approach, where Y_e, τ, and S are free parameters determined by fitting the calculated abundance pattern to the observed solar one. This approach has proven to be valuable in studying the underlying physics of the r process and, avoiding assumptions on the astrophysics site, the extracted r-process path is defined from the new experimental nuclear physics data and the abundance observations. The parameter space extracted in this way for the KTUY mass model was $Y_e = 0.30(5)$, $\tau = 80(20)$ ms, and $S_{\max} > 400$ (S in units of k_B baryon^{-1}). This space was strongly determined by the $A \approx 130$ peak, which is very sensitive to the r-process conditions. As an example, Fig. 3 shows the sensitivity of the r-process calculations to the parameter τ, for a fixed $Y_e = 0.3$. Given the parametrized astrophysical conditions, any confrontation between the resulting parameter space and the r-process site is clearly risky. However, since Y_e as low as $Y_e = 0.3$ have been recently realized in supernovae calculations [55], and since the limit $S_{\max} \approx 100$ obtained in hydrodynamical simulations of supernova explosion is still uncertain, the parameter space extracted in this study is compatible with high entropy neutrino-driven wind in core-collapse supernovae models. The features of the resulting r process were very similar to those reported in Ref. [54], which is an in-depth study of the model. Calculations were also carried out in the parameter space resulting from the merging neutron stars calculation of Ref. [15]. In this case, the r process is a superposition of Y_e components in the range $Y_e = 0.1$–0.4 and of entropy $S \sim 20$.

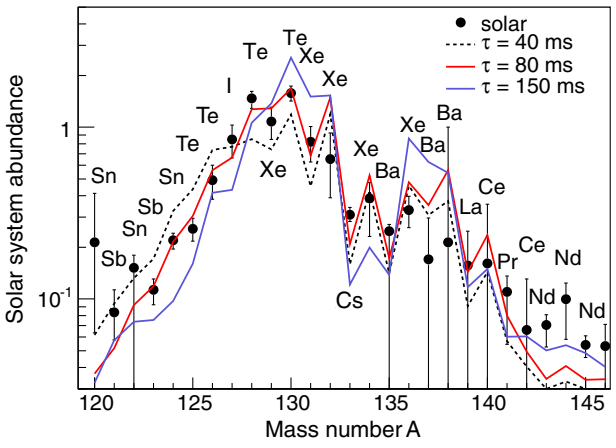

FIG. 3 (color online). Comparison between the solar r-process abundance distribution and reaction-network abundance calculations for different values of the expansion time τ.

Implications for the r process.—The impact of the new measurements on the calculated solar-abundance pattern is illustrated in Fig. 4, where two calculations are compared that differ only by the half-lives measured in this work. All the other nuclear structure data, as well as the astrophysics conditions, were the same. The new half-lives have a global impact on the calculated r-process abundances, and alleviate the underproduction of isotopes just below and above the $A \approx 130$ peak, which in the past required the introduction of shell-structure modifications [56–58]. A particularly beneficial effect of the new half-lives of the most neutron-rich isotopes of Ag, Cd, In, and Sn ($N > 82$), is to greatly improve the description of the abundance of rare earth elements, which is a prerequisite for studying the universality of the r process. The abundances of these elements are, in fact, coherently matching solar system and metal-poor stars.

The reduced nuclear physics uncertainty provides a new level of reliability for r-process calculations and their parametrized astrophysical conditions. In our calculations, the $A \approx 130$ and the rare-earth elements peaks are produced mostly in $(n,\gamma) \rightleftarrows (\gamma,n)$ equilibrium, in agreement with Ref. [54]. Thus, the large beneficial impact of the

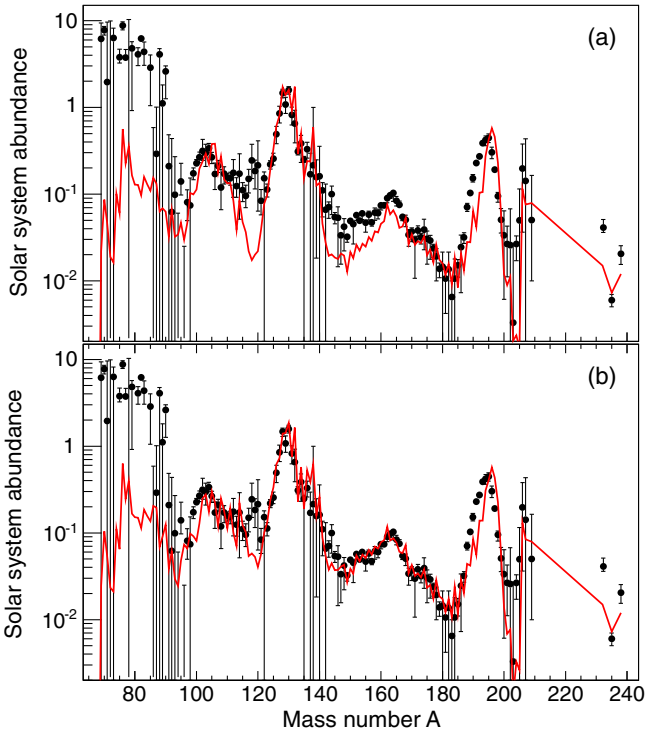

FIG. 4 (color online). Comparison between the r-process solar-system abundance pattern [18] and the abundances calculated (a) without and (b) with our new half-lives. In both calculations, we input masses from the KTUY mass model [41] and reaction rates from the ReaclibV1 library [59]. The half-lives, other than the ones we measured, are from the FRDM + QRPA model [40].

experimental half-lives on *r*-process calculations supports the notion that the observed *r*-process abundance pattern may result from the freeze-out of an $(n,\gamma) \rightleftarrows (\gamma,n)$ equilibrium. When using the FRDM mass model in the same astrophysical conditions, the *r*-process path moves to more neutron-rich nuclei. However, when calculations are fit to the solar abundance, they result in modified astrophysical conditions, which partially compensate the *r*-process path differences due to different mass models. As a result, the effect of the new half-lives in the *r*-process calculations using KTUY and FRDM mass models are the same. A similar conclusion was drawn using the Hartree-Fock-Bogoliubov mass model HFB-14 [60].

The solar system abundance pattern shown in Fig. 4 comprises contributions from many *r*-process events accumulated over time, and consequently, such pattern may be an average one. In contrast, the photospheres of metal poor stars display the output of individual or very few *r*-process events since they belong to the earlier generation of stars. As mentioned in the introduction, recent observations for a number of metal poor stars demonstrated a robust production of Te [21,22]. To study whether this finding implies the robustness of physical conditions in the *r*-process site, we calculated elemental abundances for a range of parameters $\tau = 10$–300 ms, corresponding to different *r*-process conditions (different stars). As shown in Fig. 5, in all cases, Te is, indeed, robustly produced in agreement with observation. Note, however, in the case of Te, four stable isotopes are produced by the *r* process. Although different *r*-process conditions shift the $A \approx 130$ peak of the isotopic abundance distribution (compare Fig. 3) causing variations in the abundance of the different Te isotopes, these changes compensate each other leading to a robust elemental abundance of Te. However, the situation is different for the odd-Z elements I and Cs that only have one stable isotope (^{127}I and ^{133}Cs) and for Sn that lies on the tail of the peak. In these cases, the elemental abundances retain their sensitivity to the *r*-process conditions. We conclude that (i) the robustness of Te is hard to connect to the robustness of the *r*-process conditions and (ii) the robustness of Te has a different nature than the one of rare earth elements, whose robustness was also found at the level of isotopic abundance distributions. Furthermore, (iii) the elements Sn, Sb, I, Cs in metal-poor stars are sensitive to the *r*-process conditions, and consequently, the detection of these elements could provide new stringent constraints on individual *r*-process events.

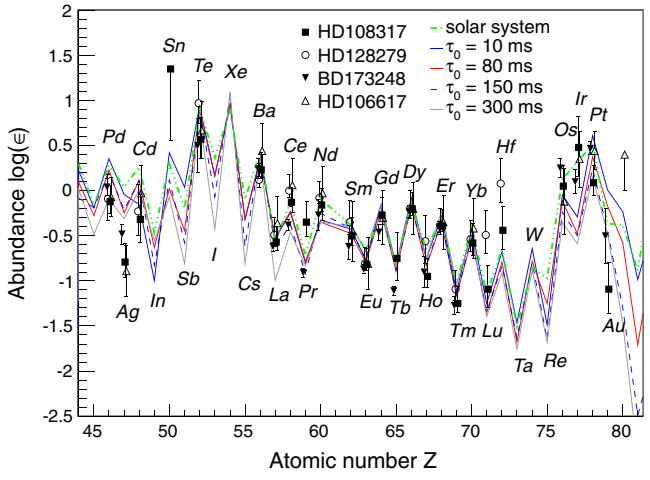

FIG. 5 (color online). Comparison between the elemental *r*-process abundance distributions in four metal-poor stars [21,22], in the solar system, and calculated for a range of *r*-process conditions. All abundance distributions are normalized to the element Eu.

In the case of calculations for merging neutron stars, the impact of the new half-lives was found to be very small because the very short expected expansion time ($\tau \sim 10$ ms) drove the *r*-process path into more exotic regions. A larger, but nevertheless modest, impact was found in the case of larger expansion times ($\tau > 100$ ms), which is relevant for the *r* process in the accretion disk around the black-hole remnant of binary neutron stars or a neutron star-black hole merger [61].

Conclusions.—The present study extends the limits of known β-decay half-lives to nuclei deep into the *r*-process path predicted for some of the most promising *r*-process sites such as neutrino-driven wind in core-collapse supernovae. The study demonstrates the persistence of shell effects and robust half-lives systematics. The comparison to predictions of theoretical models shows no evidence of structural changes capable of substantially modifying the gross properties of the nuclei studied. Reaction-network calculations based on the new data reinforce the notion that the *r*-process abundance pattern may result from the freeze-out of an $(n,\gamma) \rightleftarrows (\gamma,n)$ equilibrium, and highlight the remarkable value of abundance observations in metal-poor stars and, in particular, of Te and the other elements contributing to the $A \approx 130$ *r*-process peak. The sensitivity of these elements to the *r*-process conditions may enable metal-poor star observations to identify the exact conditions that triggered an individual *r*-process event.

This work was carried out at the RIBF operated by RIKEN Nishina Center, RIKEN and CNS, University of Tokyo. The authors acknowledge discussion with Dr. Richard Cyburt, Dr. Alfredo Estradé Vaz, Dr. Fernando Montes, Dr. Shinya Wanajo, and Dr. Volker Werner. We also acknowledge the EUROBALL Owners Committee for the loan of germanium detectors and the PreSpec Collaboration for the readout electronics of the cluster detectors. Part of the WAS3ABi was supported by the Rare Isotope Science Project which is funded by the Ministry of Education, Science, and Technology (MEST) and National Research Foundation (NRF) of Korea. This work was partially supported by KAKENHI (Grants No. 25247045, No. 2301752, and No. 25800130), the RIKEN Foreign Research Program, the Spanish Ministerio de Ciencia e

Innovación (Contracts No. FPA2009-13377-C02 and No. FPA2011-29854-C04), the U.S. Department of Energy, Office of Science, Office of Nuclear Physics, Contract No. DE-AC02-06CH11357, the NASA Grant No. NNX10AH78G, and the Hungarian Scientific Research Fund OTKA Contract No. K100835.

[1] F. Käppeler, H. Beer, and K. Wisshak, Rep. Prog. Phys. **52**, 945 (1989).
[2] F. Käppeler, R. Gallino, S. Bisterzo, and W. Aoki, Rev. Mod. Phys. **83**, 157 (2011).
[3] F. Hoyle, W. A. Fowler, G. R. Burbidge, and E. M. Burbidge, Science **124**, 611 (1956).
[4] K. Sato, Prog. Theor. Phys. **51**, 726 (1974).
[5] J. J. Cowan, F.-K. Thielemann, and J. W. Truran, Phys. Rep. **208**, 267 (1991).
[6] M. Arnould, S. Goriely, and K. Takahashi, Phys. Rep. **450**, 97 (2007).
[7] S. E. Woosley and R. D. Hoffman, Astrophys. J. **395**, 202 (1992).
[8] K. Takahashi, J. Witti, and H.-T. Janka, Astron. Astrophys. **286**, 857 (1994).
[9] C. L. Fryer, F. Herwig, A. Hungerford, and F. X. Timmes, Astrophys. J. **646**, L131 (2006).
[10] S. Wanajo, M. Tamamura, N. Itoh, K. Nomoto, Y. Ishimaru, T. C. Beers, and S. Nozawa, Astrophys. J. **593**, 968 (2003).
[11] A. G. W. Cameron, Astrophys. J. **562**, 456 (2001).
[12] C. Winteler, R. Käppeli, A. Perego, A. Arcones, N. Vasset, N. Nishimura, M. Liebendörfer, and F.-K. Thielemann, Astrophys. J. Lett. **750**, L22 (2012).
[13] J. A. Faber and F. A. Rasio, Living Rev. Relativity **15**, 8 (2012).
[14] O. Korobkin, S. Rosswog, A. Arcones, and C. Winteler, Mon. Not. R. Astron. Soc. **426**, 1940 (2012).
[15] S. Wanajo, Y. Sekiguchi, N. Nishimura, K. Kiuchi, K. Kyutoku, and M. Shibata, Astrophys. J. Lett. **789**, L39 (2014).
[16] C. Freiburghaus, S. Rosswog, and F.-K. Thielemann, Astrophys. J. **525**, L121 (1999).
[17] S. Wanajo, Astrophys. J. **666**, L77 (2007).
[18] S. Goriely, Astron. Astrophys. **342**, 881 (1999).
[19] H. R. Jacobson and A. Frebel, J. Phys. G **41**, 044001 (2014).
[20] C. Sneden, J. J. Cowan, and R. Gallino, Annu. Rev. Astron. Astrophys. **46**, 241 (2008).
[21] I. U. Roederer, J. E. Lawler, J. J. Cowan, T. C. Beers, A. Frebel, I. I. Ivans, H. Schatz, J. S. Sobeck, and C. Sneden, Astrophys. J. **747**, L8 (2012).
[22] I. U. Roederer, J. E. Lawler, J. S. Sobeck, T. C. Beers, J. J. Cowan, A. Frebel, I. I. Ivans, H. Schatz, C. Sneden, and I. B. Thompson, Astrophys. J. Suppl. Ser. **203**, 27 (2012).
[23] A. Arcones and G. Martínez-Pinedo, Phys. Rev. C **83**, 045809 (2011).
[24] H. Watanabe *et al.*, Phys. Rev. Lett. **111**, 152501 (2013).
[25] H. Wang *et al.*, Phys. Rev. C **88**, 054318 (2013).
[26] H. Watanabe *et al.*, Phys. Rev. Lett. **113**, 042502 (2014).
[27] P.-A. Söderström *et al.*, Phys. Rev. C **88**, 024301 (2013).
[28] J. Taprogge *et al.*, Phys. Rev. Lett. **112**, 132501 (2014).
[29] A. Jungclaus *et al.*, Phys. Rev. Lett. **99**, 132501 (2007).
[30] I. Dillmann *et al.*, Phys. Rev. Lett. **91**, 162503 (2003).
[31] S. Nishimura, Prog. Theor. Exp. Phys. **2012**, 030000 (2012).
[32] P.-A. Söderström *et al.*, Nucl. Instrum. Methods Phys. Res., Sect. B **317**, 649 (2013).
[33] Y. Shimizu *et al.* (to be published).
[34] Z. Y. Xu *et al.*, Phys. Rev. Lett. **113**, 032505 (2014).
[35] G. Audi, F. G. Kondev, M. Wang, B. Pfeiffer, X. Sun, J. Blachot, and M. MacCormick, Chin. Phys. C **36**, 1157 (2012).
[36] X. Zhang, Z. Ren, Q. Zhi, and Q. Zheng, J. Phys. G **34**, 2611 (2007).
[37] I. N. Borzov, J. J. Cuenca-García, K. Langanke, G. Martínez-Pinedo, and F. Montes, Nucl. Phys. **A814**, 159 (2008).
[38] T. Björnstad *et al.*, Nucl. Phys. **A453**, 463 (1986).
[39] M. Hannawald *et al.*, Phys. Rev. C **62**, 054301 (2000).
[40] P. Möller, B. Pfeiffer, and K.-L. Kratz, Phys. Rev. C **67**, 055802 (2003).
[41] H. Koura, T. Tachibana, M. Uno, and M. Yamada, Prog. Theor. Phys. **113**, 305 (2005).
[42] T. Tachibana, M. Yamada, and Y. Yoshida, Prog. Theor. Phys. **84**, 641 (1990).
[43] J. J. Cuenca-Garcıa, G. Martınez-Pinedo, K. Langanke, F. Nowacki, and I. N. Borzov, Eur. Phys. J. A **34**, 99 (2007).
[44] Q. Zhi, E. Caurier, J. Cuenca-García, K. Langanke, G. Martínez-Pinedo, and K. Sieja, Phys. Rev. C **87**, 025803 (2013).
[45] B. Fogelberg *et al.*, Phys. Rev. C **70**, 034312 (2004).
[46] M. Hannawald *et al.*, Nucl. Phys. **A688**, 578 (2001).
[47] K.-L. Kratz, B. Pfeiffer, F.-K. Thielemann, and W. B. Walters, Hyperfine Interact. **129**, 185 (2000).
[48] G. Martínez-Pinedo, A. Poves, E. Caurier, and A. P. Zuker, Phys. Rev. C **53**, R2602 (1996).
[49] C. B. Hinke *et al.*, Nature (London) **486**, 341 (2012).
[50] M. J. Bojazi and B. S. Meyer, Phys. Rev. C **89**, 025807 (2014).
[51] B. Meyer, Nuclei in the Cosmos (NIC XII) (2012) 96.
[52] I. V. Panov and H.-T. Janka, Astron. Astrophys. **494**, 829 (2009).
[53] C. Freiburghaus, J.-F. Rembges, T. Rauscher, E. Kolbe, F.-K. Thielemann, K.-L. Kratz, B. Pfeiffer, and J. J. Cowan, Astrophys. J. **516**, 381 (1999).
[54] K. Farouqi, K.-L. Kratz, B. Pfeiffer, T. Rauscher, F.-K. Thielemann, and J. W. Truran, Astrophys. J. **712**, 1359 (2010).
[55] M.-R. Wu, T. Fischer, L. Huther, G. Martínez-Pinedo, and Y.-Z. Qian, Phys. Rev. D **89**, 061303 (2014).
[56] K.-L. Kratz, J.-P. Bitouzet, F.-K. Thielemann, P. Moeller, and B. Pfeiffer, Astrophys. J. **403**, 216 (1993).
[57] B. Chen, J. Dobaczewski, K.-L. Kratz, K. Langanke, B. Pfeiffer, F.-K. Thielemann, and P. Vogel, Phys. Lett. B **355**, 37 (1995).
[58] M. Bender, K. Bennaceur, T. Duguet, P. -H. Heenen, T. Lesinski, and J. Meyer, Phys. Rev. C **80**, 064302 (2009).
[59] R. H. Cyburt *et al.*, Astrophys. J. Suppl. Ser. **189**, 240 (2010).
[60] S. Goriely, M. Samyn, and J. M. Pearson, Phys. Rev. C **75**, 064312 (2007).
[61] S. Wanajo, H.-T. Janka, and B. Müller, Astrophys. J. Lett. **726**, L15 (2011).